Outgassing of Stainless Steel Vacuum Chambers and The Vacuum Pumping Performance Evaluation of a Titanium Sublimation Pump

Christian Hammill [a)]
Department of Physics and Astronomy, Wayne State University, Detroit, Michigan, 48201

Reducing material outgassing is essential to achieve an extremely high vacuum (XHV). Previous studies have shown extremely low outgassing rates from stainless steels ($\dot{Q} \approx 2\text{x}10^{-14}$ Torr•L•s^{-1}•cm^{-2}) after they have been baked at 400°C in either a vacuum or air. This first project re-examines stainless steel outgassing rates on a pretreated (baked) stainless steel chamber that has been stored properly under N_2 for ~8 months. The outgassing rate of the sample chamber is determined mainly via the rate of rise method. The results of the rate of rise method are cross checked via the throughput method. Results have indicated that the stainless steel chamber maintained its extremely low outgassing rate after long term storage.
A Titanium Sublimation Pump (TiSP) will be used to handle very large gas loads at the entrance of the beam dump for the Cornell Prototype ERL Photo-cathode injector. The second part of this study is to evaluate the vacuum pumping performance of the TiSP, specifically the pumping speed and capacity. Our results have shown the TiSP to have a maximum pumping speed of >1,000 L/s and a pumping capacity ≤25 Torr*L for H_2 gas.

I. INTRODUCTION

This REU project consists of two parts: the study of the outgassing of a stainless steel chamber that was previously treated, tested, and stored in N_2, and the pumping performance evaluation of a titanium sublimation pump (TiSP). Both projects are closely related to the R & D efforts in construction of the Cornell Prototype Photo-cathode Injector[1], whose purpose is to shape and study the properties of the electron beam, as it must fit certain characteristics for the Energy Recovery Linac (ERL).

In certain places of the ERL, like the photo-cathode, an XHV must be maintained ($\leq 10^{-12}$ Torr). Reducing material (mainly SST) outgassing is essential to achieve an XHV. Previously, outgassing properties of stainless steel vacuum chambers have been studied. It has been found that treating a stainless steel system at 400°C can dramatically reduce H_2 outgassing[2].

The goal of the first part of the project is to find whether or not this extremely low outgassing rate lasts after the treated chamber has been properly stored in N_2 for a significant period of time (nearly 8 months in this case). This is done by examining the current outgassing rate of the sample chamber and comparing it to its outgassing rate prior to storage. This is a replication of a practical scenario in which the vacuum chamber is vented for repairs and/or updates, and then parts used on the chamber are properly stored in N_2. The outgassing properties of the sample chamber were then reexamined.

The second part of this REU project deals with the vacuum pumping issue in the Cornell ERL project. After measuring the properties of the electron beam generated in the photo-cathode electron gun, the beam must be safely terminated at the aluminum beam dump (see Fig. 1). Very large gas loads (predominately H_2 gas) are generated at the beam dump due to

[a)] Electronic mail: AQ7233@wayne.edu

electron induced desorption at the aluminum surface in the dump.

A large TiSP will be used together with two large ion pumps to control the H_2 gas load. The TiSP chamber was chosen as it was already within the possession of the lab. So, utilizing it will save both time and money.

In this part of this project, we will evaluate the pumping performance of the TiSP, which is known to be very effective in pumping H_2 gas[3]. The results of these tests will help to determine whether this TiSP is suitable for the application.

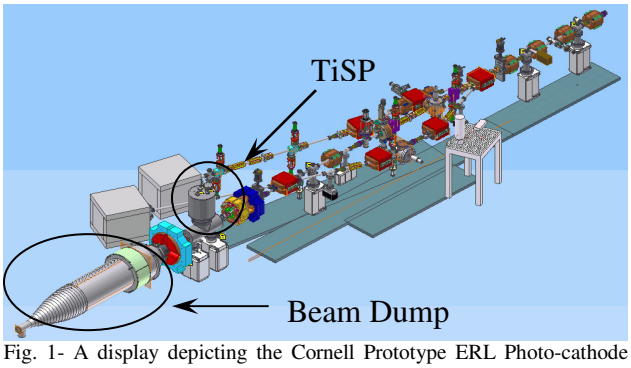

Fig. 1- A display depicting the Cornell Prototype ERL Photo-cathode injector beam line after the superconducting cavities. Marked in circles are the areas of importance to this paper, (i.e., the TiSP chamber and the Beam Dump chamber).

II. METHODOLOGY

A. Stainless steel outgassing measurements

As stated earlier, the mission of this part of the project is to re-measure the H_2 outgassing rate, $\dot{Q}$, of a stainless steel (type 314L in this case) chamber. This chamber was previously treated with a 400°C vacuum bakeout and was then stored in N_2 for ~8 months.

The outgassing measurements are carried out in a setup shown in Fig. 2. The vacuum system as a whole is divided into two parts: the testing chamber and the sensor chamber. These two components are connected through an all-metal angle valve just outside the oven. It is necessary to divide the whole vacuum system into two parts, because we need independent controls of the sensor chamber and the testing chamber. Using this setup, the stainless steel outgassing rates are measured via two methods: the rate of rise method and the throughput method.

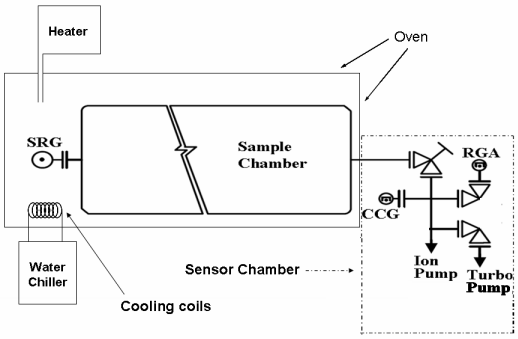

Fig. 2- A sketch depicting the outgassing vacuum system with chamber, SRG, and various vacuum components.

The testing chamber consists of the oven and all the contents contained therein. The pretreated sample (stainless steel) chamber is placed in the oven. During the rate of rise method, the temperature in the oven is controlled to within 0.1°C of a setting temperature of 25°C by aid of a combination of heating tape and water cooling coils. The heating tape and the water cooling coils are controlled outside the vacuum system via a PID controller, and the pressure in the chamber is monitored by a spinning rotor gauge, SRG.

The sample chamber and the SRG sensor head are placed inside the oven, which is designed to bake the sample chamber uniformly up to 450°C. The oven is capable of baking at this temperature by way of a high power heating gun and air blower.

The second part of the setup, the sensor chamber, consists of a cold cathode gauge, (CCG), a residual gas analyzer, (RGA), and a small ion pump. A turbo molecular pump is then connected to the sensor chamber. The sensor chamber is used for throughput measurements, determination of gas composition, and for pumping down.

In this study, the testing chamber is baked at various temperatures starting at 150°C and up to 250°C, while the sensor chamber is consistently baked at 250°C during each trial run by being

wrapped in heat tape. This temperature will eliminate water, hydrocarbons, and other carbon compounds like CO and will achieve a base pressure in the low 10^{-10} Torr range.

The pressure in the sensor chamber is monitored by the CCG. A RGA determines the makeup of the gas in the system. A turbo molecular pump is used for an initial pump-down and to handle large gas loads during bakeouts. The small ion pump is used to maintain the ultra high vacuum and for the throughput method.

The sensor chamber is made as small as possible so that its contribution to the outgassing load will be minimized.

All of the measurements, regardless of the method of choice, involve a similar procedure:

Setup and leak check: First, all of the vacuum flanges are connected properly and tightened. The entire system is then pumped down via the turbo molecular pump. Once pumped down, the system is checked for leaks with a RGA using helium as a trace gas.

Bake-out: Whenever a stainless steel vacuum system is exposed to air, water molecules adsorb onto the chamber surface. The adsorbed water must be eliminated via bakeout at temperatures ≥120°C.

The testing chamber is baked in the oven using heat gun and a hot air blower. The temperatures of both heating systems are controlled using programmable PID controllers. A typical bakeout cycle includes a smooth ramping up to a desired temperature, T_B, holding at T_B for a requested duration, and a smooth ramping down. Once the whole vacuum system has baked for a period of 48 to 72 hours, the system is left to cool and leak checked again to see if the bakeout caused any of the components in the apparatus to leak.

Measurement: When utilizing the rate of rise method, the testing chamber is isolated from the sensor chamber, and the SRG is used to measure the pressure in the testing chamber. When utilizing the throughput method, the valve to the testing chamber opens to the sensor chamber, and the pressure is measured with a CCG. The makeup of the gas is then determined using a RGA.

Both the CCG and SRG controllers are interfaced to a PC with a 12-bit data acquisition card (National Instruments© DAQ-1200). The recorded analog output voltages, V^{out} (in volts) of both gauges are later converted into the gauge pressure (in torr) using the following:

$$P_{SRG}=1x10^{-6}\bullet 10^{V_{SRG}^{out}\bullet 0.2} \quad (1)$$

$$P_{CCG}=10^{V_{CCG}^{out}/0.6-12} \quad (2)$$

Repeat: This series of steps is repeated, only each time, the baking temperature is raised. The first time this cycle of steps was ran, the baking was 150°C. It was then was raised to 200°C in the next cycle and then to 250°C in the last cycle. These repetitions, which only vary by the baked temperature, help to ensure accuracy of the data.

A1. Rate of Rise Method

In the rate of rise method, the (stainless steel) sample chamber is completely closed off to allow gas accumulation. Without any pumping in the testing chamber, and assuming a constant outgassing rate, $\dot{Q}$, the accumulation of the outgassing should result in a linear pressure increase over time, that is, a constant rate of rise in pressure, $\dot{P}$. The outgassing rate, $\dot{Q}$, can be calculated by:

$$\dot{Q} = \dot{P}\bullet V/A_s \quad (3)$$

Where V is the volume of the chamber (28 L) and A_s is the inner surface area of the chamber (7500 cm^2).

The SRG[4] is chosen for the rate of rise method primarily because the gauge does not alter (or disturb) the vacuum to be measured. This is distinctly different from the other types of gauges (such as the cold cathode gauge,

CCG), which may introduce a small amount of pumping and/or may also cause a small outgas.

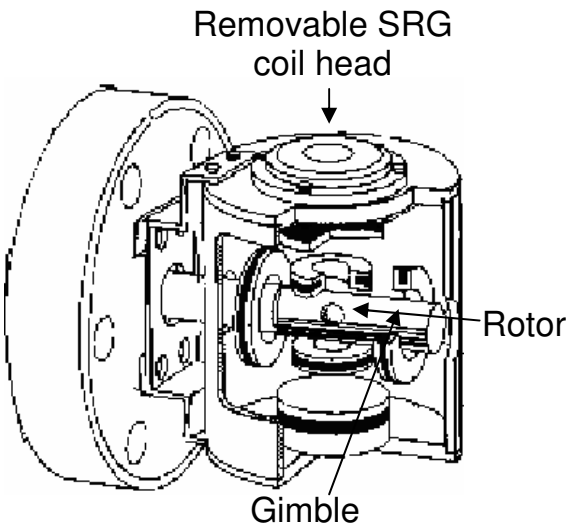

Fig. 3- The arrangement of a typical Spinning Rotor Gauge apparatus.

The SRG consists of ball (rotor) in a thimble-like chamber (see Fig. 3) in which it is suspended via a magnetic field. The rotor then begins to spin and eventually "settles" at a constant spinning frequency. Molecules in the chamber collide with the rotor, inducing a molecular drag. The amount of molecular drag on the rotor is directly proportional to the pressure inside the chamber.

It is very important that the magnetic levitation force align with gravity to ensure a stable rotor rotation. This is achieved by using a small level to adjust the orientation of the SRG head.

Other factors can affect the spinning frequency as well. For instance, temperature can cause the ball to either expand or shrink. This directly affects the inertia of the ball and therefore indirectly affects the spinning frequency of the ball. So, in all of the experiments, cooling coils and a heater (see Fig 2) were used to maintain the temperature inside the oven within $\Delta T \approx 0.1°C$ of the set temperature of 25°C.

Meaningful outgassing data was only obtained at night and/or over the weekend, because the SRG is highly sensitive to vibrations. Walking around the chamber (by lab personnel) or even lightly touching the system can cause the SRG to produce high amounts of "noise".

While these sources of error have been minimized, the SRG can only reliably measure pressure $>10^{-7}$ Torr. This is a limit set by the residual magnetic drag. In our setup, the pressure is further limited to $>10^{-6}$ Torr, due to lack of vibrational isolation to minimize ground motion. The scatter in the data is mostly caused by the residual ground vibration.

A2. Throughput method

As a cross check to the rate of rise method, the throughput method is employed. This method uses a change in pressure, ΔP (as explained later) and the pumping speed of the ion pump, S_{ip}, such that:

$$\dot{Q} = \Delta P \bullet S_{ip}/A_s \qquad (4)$$

Using a CCG and having the chamber sealed, we measure a baseline pressure in the sensor chamber. Then the testing chamber is opened to the sensor chamber to pump out the accumulated gas, and the pressure is allowed to settle to equilibrium. The absolute difference between the settled pressure and the baseline pressure is then recorded as our ΔP. Upon opening the valve between the testing chamber and the sensor chamber, the accumulated gas (predominately H_2; see Fig. 4b)) in the testing chamber is quickly pumped away by the ion pump, as shown in Fig. 4a). This pump down curve, i.e. pressure vs. time, can be fitted by the following[6]:

$$f(t) = P_o + P_1 e^{\Delta t/\tau_1} + P_2 e^{\Delta t/\tau_2} \qquad (5)$$

Where, P_o, P_1, P_2, τ_1, and τ_2 are fitting parameters (See Appendix).

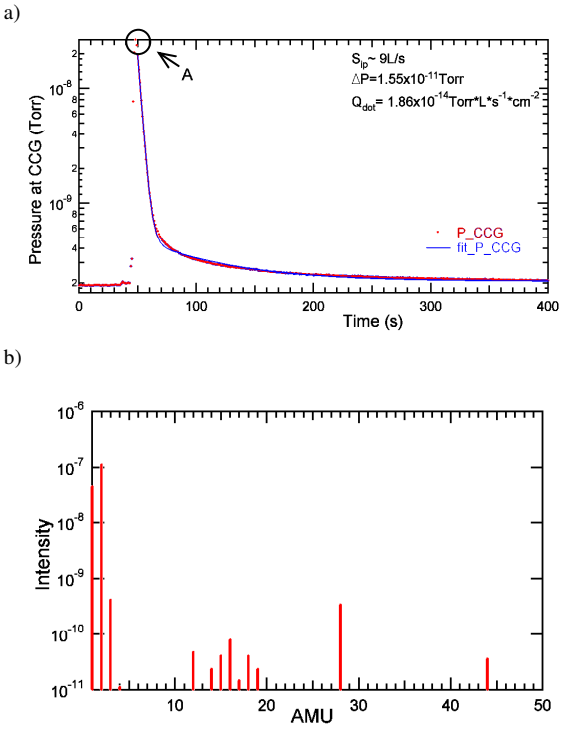

Fig. 4- a) Typical pump down curve as measured by the CCG
b) The mass spectrum of gas at the beginning of the pump down (marked as point A in a)). This shows the dominance of H_2 gas.

The pumping speed of the ion pump, S_{ip}, can be experimentally determined by analyzing the pumping down transient. One can relate the S_{ip} to the fitted τ_1 as:

$$S_{ip}=V/\tau_1 \qquad (6)$$

It is worth noting that the pumping speed determined in this way is independent of gauge calibration.

B. Determination of TiSP vacuum properties

In previous sections, it was mentioned that the purpose of the TiSP is to capture a large gas load generated in the aluminum beam dump. In Fig. 5, one can see when the beam is dumped, it causes in increase in pressure of up to ~2x10^{-5} Torr. In order to control this pressure increase and to control the gas load, a TiSP along with 2 ion pumps were placed in the A5 section.

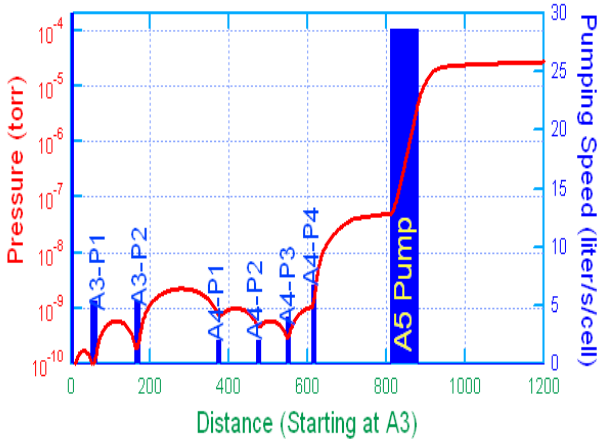

Fig. 5- The calculated[5] pressure distribution along the ERL Beamline, given the conditions that the A5 pumping speed=2000L/s and electron induced desorption yield, Y_{EID}=0.1. See also Fig 1.

To see if this TiSP is enough to handle a gas load of this sort, tests were ran to evaluate the pumping speed and capacity of the TiSP with a setup seen in Fig. 6.

Sublimation Titanium Pumps have been used in the past to capture gas loads[7] because of the high reactivity of the Titanium that coats the inner surface.

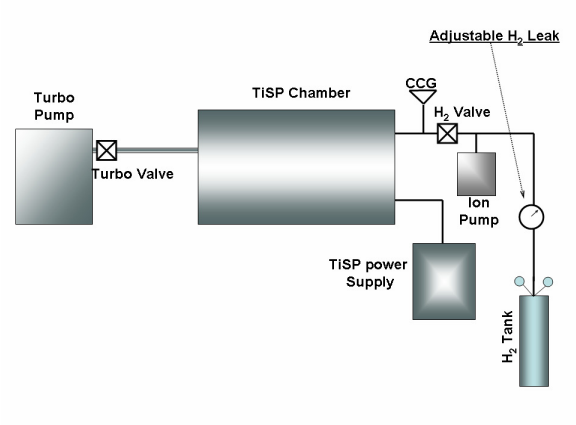

Fig. 6- Setup of TiSP chamber and vacuum apparatus.

This is an intricate process. First, the system is leak checked and then baked at 170°C. Any leak and/or contamination gas will significantly affect H_2 pumping measurements. Once cooled, a gas load of H_2 is introduced into the chamber via an adjustable leak. Before any Ti sublimation, the H_2 leak rate, $\dot{Q}$, is measured by flowing the H_2 gas through the TiSP chamber

into the turbo. The small ion pump is turned off during the leak rate measurements.

With a known turbo pumping speed, S_{turbo}, and the measured pressure at the turbo, P_{turbo}, the leak rate can be calculated as:

$$\dot{Q} = 2.4 \bullet S_{turbo} \bullet P_{turbo} \quad (7)$$

Where the factor of 2.4 is to correct the gauge sensitivity to H_2.

As shown later, it is necessary to determine the effective turbo pumping speed at the location of the CCG, S_{turbo}^{eff}. This is done so by using a similar formula to Eq. (7):

$$S_{turbo}^{eff} = \dot{Q} / (P_{CCG}^{C} \bullet 2.4) \quad (8)$$

Where P_{CCG}^{C} is the pressure at the CCG before any Ti sublimation.

After these measurements have been made, the H_2 leak valve is closed and the ion pump is turned on (to avoid any H_2 build up). The Ti is then sublimated into the chamber by heating the Ti filaments resistively via a power supply. This process is called "flashing". The flashing process takes place at a certain power level and for a certain period of time. The longer the sublimation time and/or the higher the power used for sublimation, the thicker the Ti layer. After the flashing process, the pressure will recover.

Once the pressure has recovered, the H_2 leak valve is reopened and the ion pump is turned back off to let the gas flow though the chamber (to saturate the Ti coating) and into the turbo pump. The pressures at the CCG and at the turbo will now vary with time and are recorded as $P_{CCG}(t)$ and $P_{Turbo}(t)$ respectfully.

The pumping speed acting at the location of the CCG is the sum of the effective pumping speed of the turbo, S_{turbo}^{eff}, and the pumping speed of the TiSP, $S_{Ti}(t)$. Using a similar relation as seen in Eq. (7), one finds:

$$\dot{Q} = 2.4 \bullet (S_{turbo}^{eff} + S_{Ti}(t)) \bullet P_{CCG}(t) \quad (9)$$

As time goes on, the Ti layer becomes more and more saturated with H_2, which causes the $S_{Ti}(t)$ to decrease.

$$S_{Ti}(t) = \frac{\dot{Q}}{P_{CCG}(t)} - S_{turbo}^{eff} \quad (10)$$

Once the Ti layer becomes saturated with H_2, one can repeat the flashing process again. Only limited Ti flashing and H_2 saturation cycles were done, as thick H_2 rich/Ti thin films are known to be "flaky"[8].

The amount of H_2 pumped by the Ti film can be calculated as:

$$Q(t) = \int_0^t [S_{Ti}(t_j) \bullet P_{CCG}(t_j)] dt_j \quad (11)$$

Or practically,

$$Q(t) = \sum_{t=0}^{t} [S_{Ti}(t_j) \bullet P_{CCG}(t_j)] \Delta t_j \quad (12)$$

Where $1/\Delta t$ is the sampling rate and $\Delta t_j = 10s$.

III. RESULTS

A. Stainless Steel Outgassing Results

All of the rate-of-rise measurements were taken with the SRG under a stabilized oven temperature and during "quiet" evening and/or weekend hours. A typical rate of rise measurement is shown in figure 7a) along with the corresponding stable oven temperature (7b)). A linear pressure rise over time is clearly observed in 7a). The fitted slope, dP/dt, is then used to calculate the outgassing, $\dot{Q}$, using Eq. (3). Measurements of $\dot{Q}$ using the rate of rise

a)

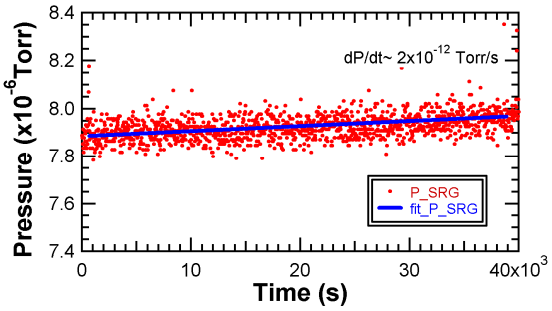

b)

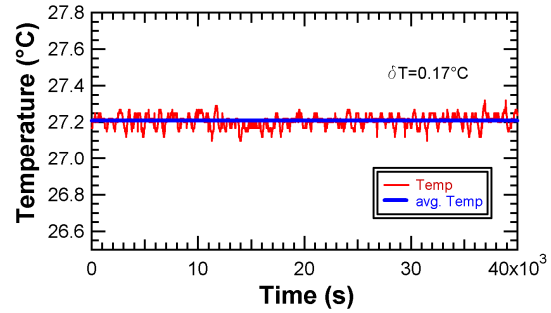

Fig. 7- a) Pressure change inside the sample chamber after a 120°C moisture elimination bake as recorded by the SRG with a slope, dP/dt ≈ $2x10^{-12}$ Torr/s.

b) The stabilized temperature (δT=0.17°C) corresponding to the same span of time as the pressure graph above.

method were taken with the testing chamber baked at 120°C, 150°C, 200°C, and 250°C.

To further confirm the outgassing rates determined by the rate of rise method, the throughput method was employed. In order to do so however, one needed to derive the pumping speed of the ion pump S_{ip}. Using Eq. 5 and similar data to that found in Fig. 4a), S_{ip} was derived to be ~9 L/s. Once S_{ip} is determined, $\dot{Q}$ can be derived using Eq. (4).

Table 1 summarizes the results from both methods (the throughput when available). For comparison, measured outgassing rates for the same sample chamber 8 months ago[9] were given.

a)

Summary Data from This Project

T_{Bake} (°C)	$\dot{Q}$ (10^{-15} Torr•L•s^{-1}•cm^{-2})	
	Rate of Rise	**Throughput**
120	2.6	30
	6.0	19
	7.5	n/a
150	25	n/a
	18	n/a
	15	n/a
200	6.7	15
	6.7	28
250	9.3	35
	7.5	38

b)

8 months ago, after 400°C Bake

T_{Bake} (°C)	**$\dot{Q}$ (10^{-15} Torr•L•s^{-1}•cm^{-2})**
150	19.0
200	16.0
250	14.0

Table 1- The above tables are summaries of the outgassing rates of the stainless steel sample chamber both currently (a) and 8 months ago (b). In table a), some measurements were taken multiple times over multiple dates, but the measurements were all taken from the same bakeout.

As one can see from comparing the results of table 1, the outgassing rates measured in this study are comparable with the results from 8 months ago. This indicates that the extremely low outgassing property can be maintained.

The comparison between the rate of rise method and the throughput results is very good, when one considers at least two factors:

1) The measurements were done at very different pressure ranges (~10^{-6} torr for rate of rise, and ~10^{-10} torr for the throughput).
2) They both use very different gauges.

B TiSP vacuum performance results

The pumping speed of the TiSP is measured at two Ti-flashing settings; (A) for 3 minutes at 170W and (B) for 5 minutes at 195W (see Fig. 8). Higher Ti-flashing power with longer duration resulted in a much thicker Ti layer. The calculated pumping speeds (using Eq. (10)) are plotted against the pumped amount of H_2 (using Eq. (12)). Both curves in Fig. 8 showed a very similar H_2 saturation trend. After an initial sharp rising in $S_{Ti}(t)$, the TiSP remains at a relatively constant pumping speed and then falls rapidly when the Ti coating is near full saturation.

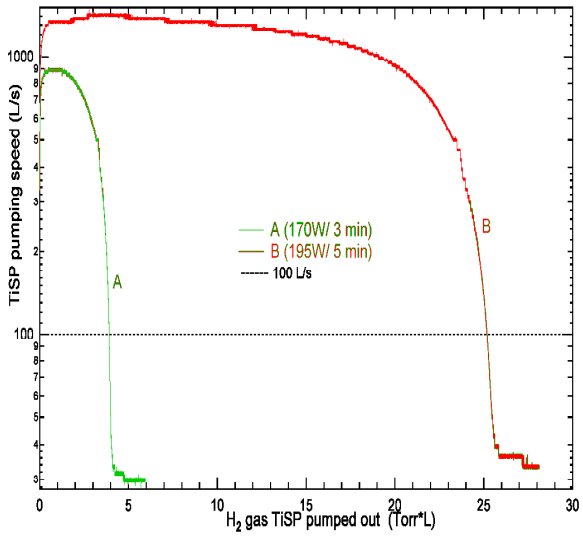

Fig. 8- Pumping speed of the TiSP vs. the amount of H_2 gas pumped at two Ti-flashing conditions: A: 170W/ 3 minutes and B: 195W/ 5 minutes.

One can see the dramatic increase in the pumping performance of the TiSP (nearly 5 times the amount of H_2 in the thicker Ti layer). This is explained when one looks at the process that H_2 undergoes when it is inside the TiSP chamber.

H_2 pumping on Ti films undergoes two steps: first, H_2 reacts with the surface layer of Ti so strongly that its diatomic bond is broken and 2H atoms are adsorbed onto the surface. This first step is known as dissociative adsorption. Next, the adsorbed H atoms are then diffused into the bulk of the thin Ti film. This process is known as bulk diffusion. The first step of the H_2 pumping is strongly dependant on the Ti surface reactivity, while the second step is affected by the H content in the thin Ti film.

The much higher pumping capacity measured on the thicker Ti coating reflects the bulk-pumping. It also indicated that the chamber is under a very clean vacuum (from good vacuum practice and bakeout) and a high purity H_2 source. Any contamination will "poison" the surface layer of Ti. When the surface layer of the Ti is "poisoned", then this stops the first step of dissociative adsorption, thus stopping the H_2 pumping.

One important practical parameter of the TiSP pumping performance is its pumping capacity, Q, which is the amount of gas (H_2 here) pumped that reduces the pumping speed to an unacceptable level for a particular application. By definition, Q is relatively arbitrary and depends on its application. Here, we chose Q to be the point where $S_{Ti}(t)$ drops to ~100L/s (i.e. ~10% of its initial pumping speed). With this definition, one sees from Fig. 8 that:

$Q_A \approx 4$ Torr•L
$Q_B \approx 25$ Torr•L

It is worth mentioning here that it took more than 80 hours of H_2 pumping in curve B to reach the saturation.

IV. CONCLUSIONS

It was the purpose of the first part of this REU project to see if a pretreated chamber stored in N_2 for a period ~8 months maintained its extremely low outgassing rate ($<2\times10^{-14}$ Torr•L•s^{-1}•cm^{-2}). The data given in Table 1 clearly indicates that a simple moisture elimination bakeout (i.e. $T_{bake} \geq 120°C$) can achieve the extremely low outgassing rates, even when the treated SST has been stored for long periods of time.

Therefore in certain places in the ERL, like the photo-cathode, one can vent out the vacuum, properly store the stainless steel components in N_2, and not have to worry about damaging the outgassing properties of these components.

With regard to the second part of this project, it can be seen from Fig 8 that the pumping speed of the TiSP is >1,000 L/s for H_2 gas and that it is capable of pumping out ≤25 Torr•L of H_2 gas. As seen from Fig. 5, the estimated gas load at the A5 section of the Cornell Proto-type Photo-cathode Injector can be as high as 1.8×10^{-3} Torr•L/s. Considering that two other ion pumps will be sharing half of the load, the TiSP will have to handle a gas load of 9.0×10^{-4} Torr•L/s. This means that the TiSP can go 7.8 hours before needing to go through a flashing cycle again. This is considered to be sufficient for the injector operations and therefore the TiSP will be installed in the A5 section.

APPENDIX

For a typical pumpdown process, with a chamber volume (V) and pumping speed (S), the pumpdown rate can be described as such:

$$\frac{d(PV)}{dt} = PS \qquad \text{(A1)}$$

We can then see that, when solved for P(t),

$$P(t) = P_o + P_1 e^{\Delta t/\tau} \qquad \text{(A2)}$$

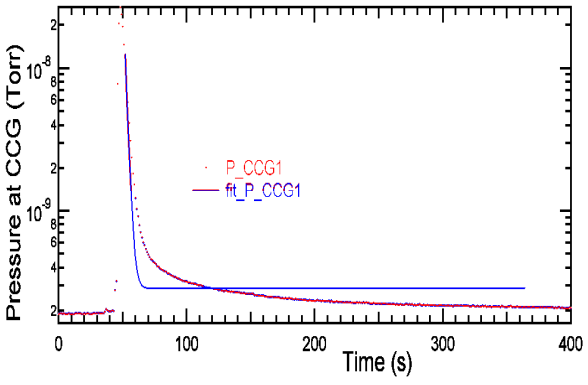

Fig. A1- Typical pumpdown curve with a fitted single exponential function.

However, one can see from Fig. A1 that a single exponential function (as suggested from Eq. (A2)) does not fit the data well. Therefore a second exponential term is introduced (see Eq. (5)).

As shown in Fig. 4a), the double exponential function (Eq. (5)) yielded a much better fit to the pumpdown curve. Though the physical nature of the second exponential term in Eq. (5) is not clear, it may indicate an additional pumping action during the pumpdown.

One suspected candidate for the additional pumping process is the H_2 re-adsorption onto the wall of the testing chamber. This is in agreement with the fact that the outgassing rates by the rate of rise method are always smaller than that measured by the throughput method. In the rate of rise measurements, the H_2 pressure is 3-4 orders of magnitude higher than in the throughput measurements; thus, higher re-adsorption rate. The higher re-adsorption rate in the rate of rise measurements resulted in lower measured outgassing rates.

ACKNOLEDGEMENTS

Thanks are due to Dr. Yulin Li and Dr. Xianghong Liu, my mentors, who have assisted me in the writing of this paper, the assembling of the experiments, and the overall guidance though this project. Special thanks should be given to the lab technician staff; Tim Giles, Tobey Moore, and Brent Johnson. Also, thanks to Dr. Rich Galik and Dr. Claude Pruneau who are the assemblers of this REU project and made it able for me to attend the summer here. Finally, thanks are due to the National Science Foundation who every year makes it possible for students much like me to have experiences like this one.

On more of a personal note, I would like to thank my Lord and Savior Jesus Christ, who everyday gives my heart another reason to beat. I would like to thank my mother who all my life, carried me “on the wings of a snow white dove”, my father, who would only accept my best, and my best friend Rich who helped to

organize my life when I needed it most and brought me to where I am at today. Also, I would like to thank my sister “Mary”, who at any moment in time, especially when I need it, can make me laugh. “Mary” also helped me in formatting this paper, of which I am eternally grateful. Finally, to my friends, family, and endless cups of coffee, I thank you all for helping me to bring the best out of me. May God bless you all.

[1]ERL Web Site URL-http://erl.chess.cornell.edu/
[2]M. Bernardini, et al., J. Vac. Sci. Technol. A **16**, 188-193 (1998).
[3]Y. Li, Y. He, and B. Mistry, J. Vac. Sci. Technol. A **21**, 1457-1459 (2003).
[4]S. K. Loyalka, J. Vac. Sci. Technol. A **14**, 2940-2942 (1996).
[5]Beamline Web Site URL-https://wiki.lepp.cornell.edu/lepp/bin/view/ERL/private/sections
[6]J. Moore, C. Davis, and M. Coplan, *Building Scientific Apparatus*, 2nd ed. (Addison-Wesley Publishing Company, Redwood City, CA, 1989), pg. 79
[7]John F. O’Hanlon, *User’s Guide to Vacuum Technology*, 2nd ed. (John Wiley & Sons, New York, NY, 1989), pgs. 237-243.
[8]R. Gibala and R. F. Hehemann, *Hydrogen Embrittlement and Stress Corrosion Cracking,* (American Society for metals, Metals Park, OH, 1992).
[9]Chongdo Park, Xianghong Liu, and Yulin Li, Private communication